

Article

Molecular TiO₂ Modifications of Supported PPh₃-Capped Pd Nanocatalysts for CO₂ Hydrogenation into Formates

María Dolores Fernández-Martínez and Cyril Godard * 

Department of Physical and Inorganic Chemistry, Universitat Rovira I Virgili, C/Marcel·lí Domingo s/n, 43007 Tarragona, Spain; mariadolores.fernandez@urv.cat

* Correspondence: cyril.godard@urv.cat; Tel.: +34-977-559574

Abstract: TiO₂-supported Pd NPs-based materials were prepared following two distinct approaches: For the first set of materials 1–8, modification of the TiO₂ support was performed prior to Pd NPs deposition, while the second set (9–15) was synthesized by deposition of modifiers over pre-synthesized Pd-PPh₃/TiO₂. These catalysts were applied in the hydrogenation of CO₂ to formate, and their performance was compared with that of the unmodified Pd-PPh₃/TiO₂. Modification of the TiO₂ support by organosilanes provided a beneficial effect in catalysis compared with the catalyst containing unmodified TiO₂ or TiO₂ modified by organophosphonic acids. In contrast, in most cases, the deposition of modifiers over previously synthesized Pd NPs supported on TiO₂ was not beneficial to the activity of the catalyst. Interestingly, upon recycling, the first set of catalysts suffered a rapid decrease in activity, while the anchoring of modifiers over previously formed Pd NPs showed an improved stability (TON > 500 after the third recycling).

Keywords: CO₂ hydrogenation; palladium; nanoparticles; catalyst modifications



Citation: Fernández-Martínez, M.D.; Godard, C. Molecular TiO₂ Modifications of Supported PPh₃-Capped Pd Nanocatalysts for CO₂ Hydrogenation into Formates. *Catalysts* **2024**, *14*, 487. <https://doi.org/10.3390/catal14080487>

Academic Editors: Bo Weng and Werner Oberhauser

Received: 20 June 2024
Revised: 17 July 2024
Accepted: 26 July 2024
Published: 29 July 2024



Copyright: © 2024 by the authors. Licensee MDPI, Basel, Switzerland. This article is an open access article distributed under the terms and conditions of the Creative Commons Attribution (CC BY) license (<https://creativecommons.org/licenses/by/4.0/>).

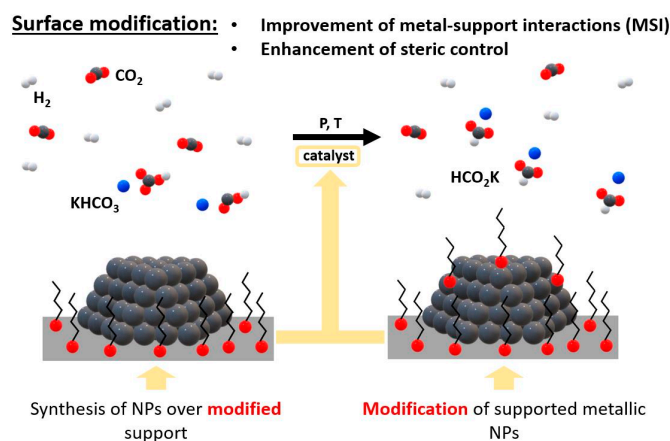
1. Introduction

The high concentration of CO₂ in the atmosphere is nowadays regarded as a critical issue and has generated a strong interest in research for the development of non-fossil-based feedstocks. As such, in spite of its inertness, CO₂ is viewed as a very attractive C1 source to produce fuels and chemicals [1–4]. Among the potential transformations of CO₂, its hydrogenation into formic acid and derivatives has become a priority in view of the recent progress made in the production of H₂ via water splitting [5]. Indeed, formic acid offers high hydrogen storage capacity and stability and provides a methodology for CO₂ storage in a chemically stable form, closing a hydrogen energy cycle [6–8].

Among the heterogeneous catalysts reported for the hydrogenation of CO₂ into formates, Pd was described as one of the most active metals [7,9–12], and the combination of Pd with other metals such as Au [8,13], Ag [14–16], and Ni was also described as efficient for this transformation [17]. The selection of the support is also significant in this process, and for instance, Pd catalysts on carbon-based supports such as reduced graphene oxide (rGO), N-doped carbon (N-C), or mesoporous graphitic carbon nitride (g-C₃N₄) provided excellent results for the hydrogenation of bicarbonates to formates [13,18]. In 2018, Mori et al. reported highly efficient CO₂ hydrogenation using Pd-based catalysts supported onto TiO₂ [16].

Heterogeneous catalysts have become a crucial part of many industrial activities, such as organic synthesis, oil refining, and pollution control [19–24]. Modern heterogeneous catalysts consist of several elements in precise proportions [21] and are optimized to obtain the greatest reaction rate, which in turn results in optimal selectivity [20–22]. The heterogeneous catalyst performance can be improved by modifying the support using approaches such as nanotechnology and nanoscience or controlling the pore structure [23–25]. However, the support must retain its specific properties, such as porosity, surface area, dispersion, selectivity, and activity [26–30].

In the design of new catalysts, the appropriate metal–support interactions (MSI) must be achieved, and their tuning can be completed through adjustments of either the composition and/or morphology of the support and active phase or through the modifications of their surface (Scheme 1) [31–34]. However, changes in composition and morphology can affect their nature [35,36]. Surface modifications can enhance steric control or provide hydrophilic/hydrophobic characteristics that can be suitable for the target substrates and catalysis media [37]. In this area, the use of organic self-assembled monolayers (SAMs) is of particular interest since these organic modifiers can act as spacers between NPs to minimize sintering and improve the stability/recyclability of the catalyst [38,39]. Moreover, depending on the functional groups in these modifiers, the catalyst activity can be enhanced through interactions with the substrate [40–42] or by conferring a hydrophobic/hydrophilic character to the system to favor catalyst–substrate interactions [43].



Scheme 1. Modifications of catalyst surface for hydrogenation of CO₂ to formates in basic media.

Modification of carbon- and silica-supported catalysts with organic molecules were previously reported to cover metallic nanoparticles with an alkylic chain [44,45] or with groups containing amine functionalities [14,46] to produce catalytic materials for CO₂ hydrogenation into formate. Organosilanes are among the most used molecules to modify supports, and they constitute a type of inorganic/organic hybrid materials [47]. Aminoalkylsilanes such as (3-aminopropyl)triethoxysilane (APTES) are the most commonly reported organosilanes [48]. Modification occurs through silanization, which is a process that covers a surface such as metal oxide with chloro or alkoxysilane [49]. Using APTES, this process starts with the hydrolysis of the ethoxy groups that are catalyzed by water, leading to the formation of silanols that condense with the surface hydroxyls to form a monolayer [50]. The most accepted chemisorption of APTES onto TiO₂ implies one or two Si–O–Ti bonds [48,51,52]. Moreover, APTES can also be applied directly over metallic nanoparticles for their stabilization and functionalization [53–55].

Liu et al. reported that APTES directly participates in the synthesis of a protonated Schiff base that covers Au NPs during the dehydrogenation of FA into CO₂ and H₂ [56]. Later, the same authors developed a new Au-based catalyst for the hydrogenation of CO₂ into formic acid in which the SiO₂ support was modified by APTES and a Schiff base, reaching a TON of 14,470 over 12 h at 90 °C [57]. The same year, Mori et al. reported PdAg NPs supported over amine-functionalized mesoporous silica for reversible CO₂ hydrogenation and release of H₂ [58]. DFT calculations revealed that the presence of amine affects the O–H dissociation of FA and favors the adsorption of CO₂ in hydrogenation. Additionally, the catalyst could be recovered and reused for three runs without loss of activity.

Srivastava reported the preparation of Ru NPs supported over various amine organosilane-modified SBA-15 mesoporous silica and their application as a catalyst in the hydrogenation of CO₂ into formic acid [59]. Primary, secondary, and tertiary amines were tested, and the use of the primary amine provided the highest catalytic activity.

Ionic liquids (ILs) constitute another type of interesting molecules for support modification [60,61], and in catalytic reactions involving CO₂, it was reported that the interactions between IL and CO₂ usually depend on the anion. Indeed, basic anions such as acetate in combination with 1,3-dialkylimidazolium enhanced such interactions [62], and this type of ILs was used in the hydrogenation of CO₂ to formic acid [63,64]. In recent years, Leitner and co-workers reported the preparation of metallic nanoparticles in ionic liquids covalently grafted onto SiO₂ by silanization [65–74]. They recently reported a Ru-based catalyst supported over an imidazolium-based supported ionic liquid phase (SILP) for the hydrogenation of CO₂ into formate in the presence of NEt₃ [75]. The authors first covalently modified the SiO₂ surface with ILs via silanization, while the synthesis of the Ru NPs was performed in a second step using the organometallic approach [76]. Modifications of the alkyl chain and anion proved very important to modulate the NPs properties and resulted in an increase in the TON by 2- or 10-fold when compared with unmodified Ru/SiO₂ catalyst. Using H/D exchange experiments, the authors determined that the modification favored the desorption of formate from the catalyst surface. However, in recycling experiments, a significant loss of activity was observed, which was attributed to the leaching of IL from the support due to the use of NEt₃ + H₂O as the solvent system. Other authors reported Pd NPs supported over poly(ionic liquid)s (PILs) for the hydrogenation of CO₂ into formic acid [77,78]. Using this catalytic system, a TOF of 1190 h⁻¹ was obtained in the presence of NEt₃ aqueous solution, and good recyclability was observed during several runs [77].

Organophosphonic acids (PAs) constitute another common type of molecules used for the modification of support surfaces. These RPO(OH)₂ compounds were especially used to modify metal oxide surfaces [79]. However, when PAs are used for surface modification, an additional annealing or aging treatment is necessary to produce condensation reactions and form strong bonds between PAs and metal oxide [39].

In a previous report from our group, ligand-capped nanocatalysts were prepared over supports of different natures (metal oxides and carbon based) and tested in Pd-catalyzed hydrogenation of CO₂ to formate. The presence of stabilizing ligands proved crucial to obtain small and well-defined Pd NP. In this study, the best performance was achieved using TiO₂-based catalysts [80]. However, upon recycling, a rapid decrease of activity was observed.

Here, modifications of the TiO₂ support/PPh₃-capped catalyst are described using Si- and P-based molecular modifiers for the first time. These new materials were characterized and tested in the catalytic hydrogenation of CO₂ into formate. The effect of these modifications on the activity and recyclability of these catalysts was particularly investigated.

2. Results and Discussion

The modified catalysts were prepared according to two distinct approaches using triethoxysilanes (TESs) and organophosphonic acids (PAs) as modifiers (Figure 1).

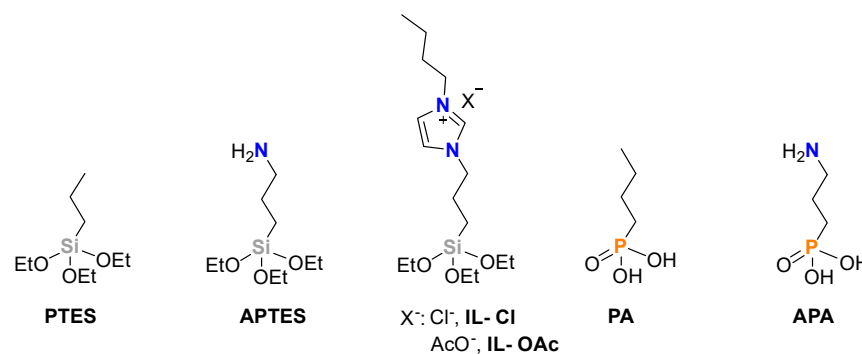
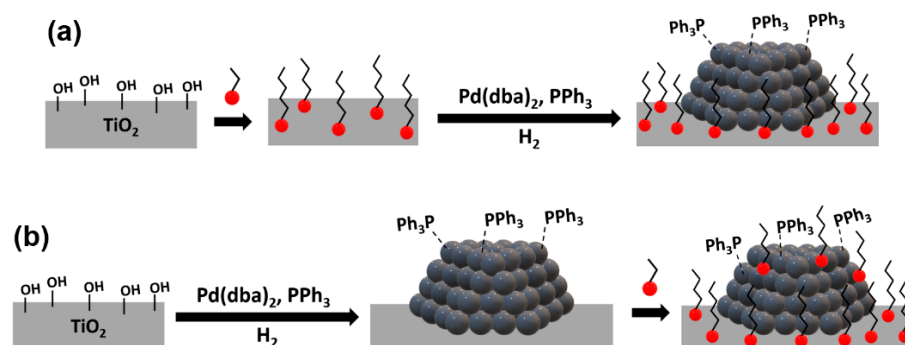


Figure 1. Modifying agents used for TiO₂ modification.

In the first approach, the TiO₂ support was modified prior to Pd NP deposition, whereas in the second approach, the Pd NPs were initially supported onto TiO₂ [80], and the modifiers were reacted subsequently (Scheme 2).



Scheme 2. Deposition of modifier on a support prior to metal catalyst formation (reverse deposition) (a) and deposition of modifier on a previously synthesized supported metal catalyst (b).

The grafting of the RSi(OEt)₃ modifiers onto TiO₂ was carried out following the literature procedures (Figure 1) [52,81]. In a typical synthesis, the reaction was performed in an EtOH:H₂O solution or absolute EtOH. The mixture was then centrifuged, and the solid was washed several times with H₂O and EtOH and dried under a vacuum for several hours.

The optimization of synthesis parameters such as concentration of APTES, APTES/TiO₂ ratio, temperature, and time was initially performed (Table S1). Organophosphonic acids (PAs) containing a butyl chain or a 3-propylamine group were also used as modifiers (Figure 1). The preparations were carried out using a modifier concentration of 0.01 M at room temperature. For these modifiers, an additional annealing or aging treatment of the material at 120 °C was performed.

To confirm the successful modification of TiO₂, the samples were first analyzed by FT-IR analysis (Figures S2, S5 and S7), which corroborated that the condensation between surface TiO₂ hydroxyl groups and silanol groups had taken place via the detection of CH₂ and C-N stretching bands.

Quantification of the anchoring of the modifiers was carried out via TGA analysis through analysis of the weight losses observed in every case (Figures S3, S6, S8 and Table S2). Apart from the low-temperature (<200 °C) weight loss associated with the removal of water, a new weight loss between 200 and 450 °C was detected for the modified TiO₂ samples and was attributed to the loss of anchored modifiers. Variations between 1 and 3.5 wt% were measured depending on the nature and concentration of modifier used.

In view of these results, it was concluded that a series of functionalized TiO₂ supports was successfully prepared using organosilanes and organophosphonic acids as modifiers. FT-IR analysis confirmed the presence of these modifiers at the surface of the TiO₂ supports (Figures S2, S5 and S7), and TGA (Figures S3, S6, S8 and Table S2) provided quantitative information about these systems.

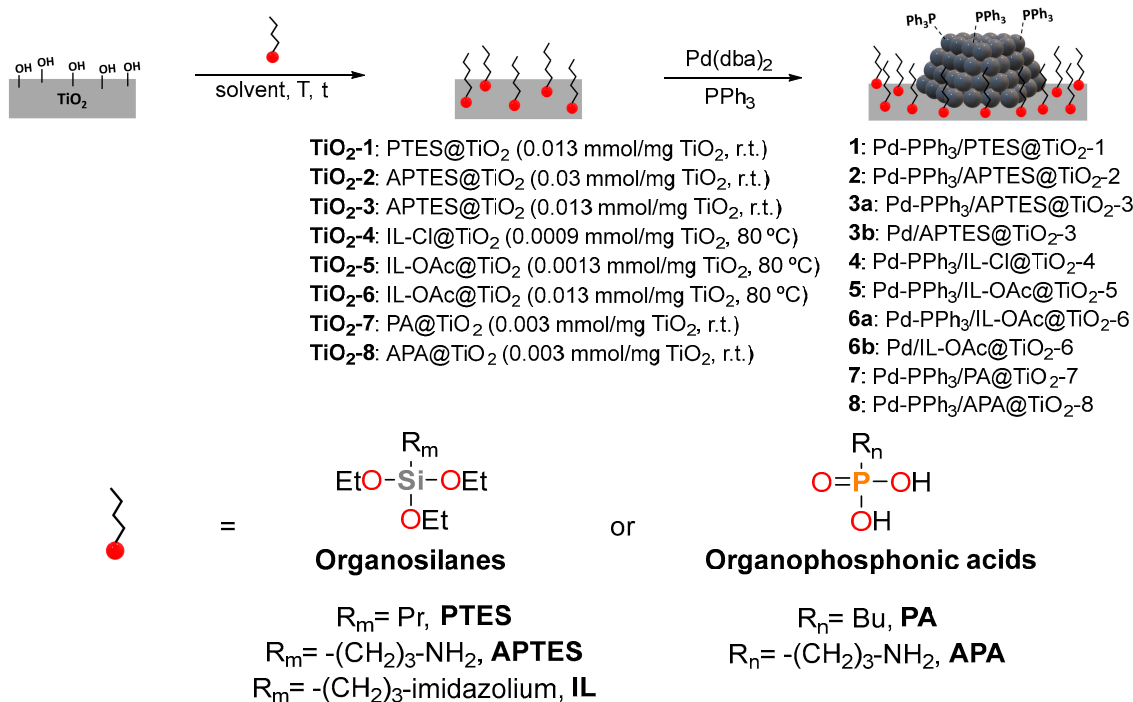
2.1. Synthesis and Characterization of Supported PPh₃-Capped Pd NPs over Modified TiO₂

The synthesis of Pd NPs was carried out over the modified TiO₂ supports in the presence of PPh₃ as the stabilizing ligand (Scheme 3). The materials were prepared by decomposition of Pd(dba)₂ under H₂ pressure at room temperature using THF as the solvent. A nominal Pd loading of 4 wt% was targeted.

The newly prepared systems were characterized by TEM, HR-TEM, ICP, XPS, FT-IR, and TGA.

Samples were analyzed by TEM to obtain information about the size and morphology of the nanoparticles. TEM images of the newly synthesized materials are displayed in Figure 2. In all cases, small and crystalline Pd NPs were formed. The sizes and distributions

obtained from TEM measurements and ICP results are summarized in Table S3. In all cases, Pd loadings between 2.7 and 3.5 wt% were measured.



Scheme 3. Synthesis of nanoparticles stabilized with PPh₃ supported over modified TiO₂.

For catalyst **1** bearing PTES as the TiO₂ modifier (Figure 2a), the resulting NPs exhibited a size of 5.75 nm with a broad distribution. Some agglomerations of Pd NPs were also observed. When TiO₂ modified with APTES was employed as support (Figure 2b–d), the Pd NPs sizes ranged from 2.04 nm to 2.52 nm, while the Pd content was between 2.75% and 3.36 wt%. The material **2** was also analyzed by HR-TEM (Figure S10) to confirm the size of the Pd NPs and obtain information on their crystallinity. EDS mapping (Figure S10c) provided information about the composition of the catalyst active phase and revealed the presence of Si at the surface of TiO₂, which confirmed the presence of APTES. The catalyst **3b** (Figure 2d), synthesized in the absence of a ligand, was also analyzed by HR-TEM (Figure S11). For this catalyst, the same edge of Si is appreciated (Figure S11c). The difference in Pd NP size observed for the PTES-modified support and those modified with APTES clearly indicated the role of the amine function in the NP stabilization. The largest NPs were obtained when the synthesis was performed in the absence of PPh₃, indicating that this ligand also played a role in the NP stabilization, although to a much lesser extent than the amine group from the support.

When the support was functionalized by organosilanes containing an IL moiety, particle sizes between ca. 1.9 and 2.4 nm were measured (Figure 2e–h). The catalyst **4** containing a support modified by IL was also analyzed by HR-TEM and EDS (Figure S12). Due to the low concentration of IL-Cl employed for synthesis of this catalyst, the layer of Si around TiO₂ was narrow. The presence of P was also observed, indicating that the ligand remained on the NPs. Interestingly, for the materials **5** and **6a**, which contain TiO₂ modified by the same organosilane but differ by the loading of organosilane at the support surface, only a slight difference in size was observed (2.43 vs. 1.99 nm). Moreover, when the synthesis of **6a** was repeated in the absence of PPh₃ **6b** (Entry 8), similar size and Pd loading were observed, indicating that the ligand was not playing an important role in the Pd NP stabilization when the IL-containing modifiers were used.

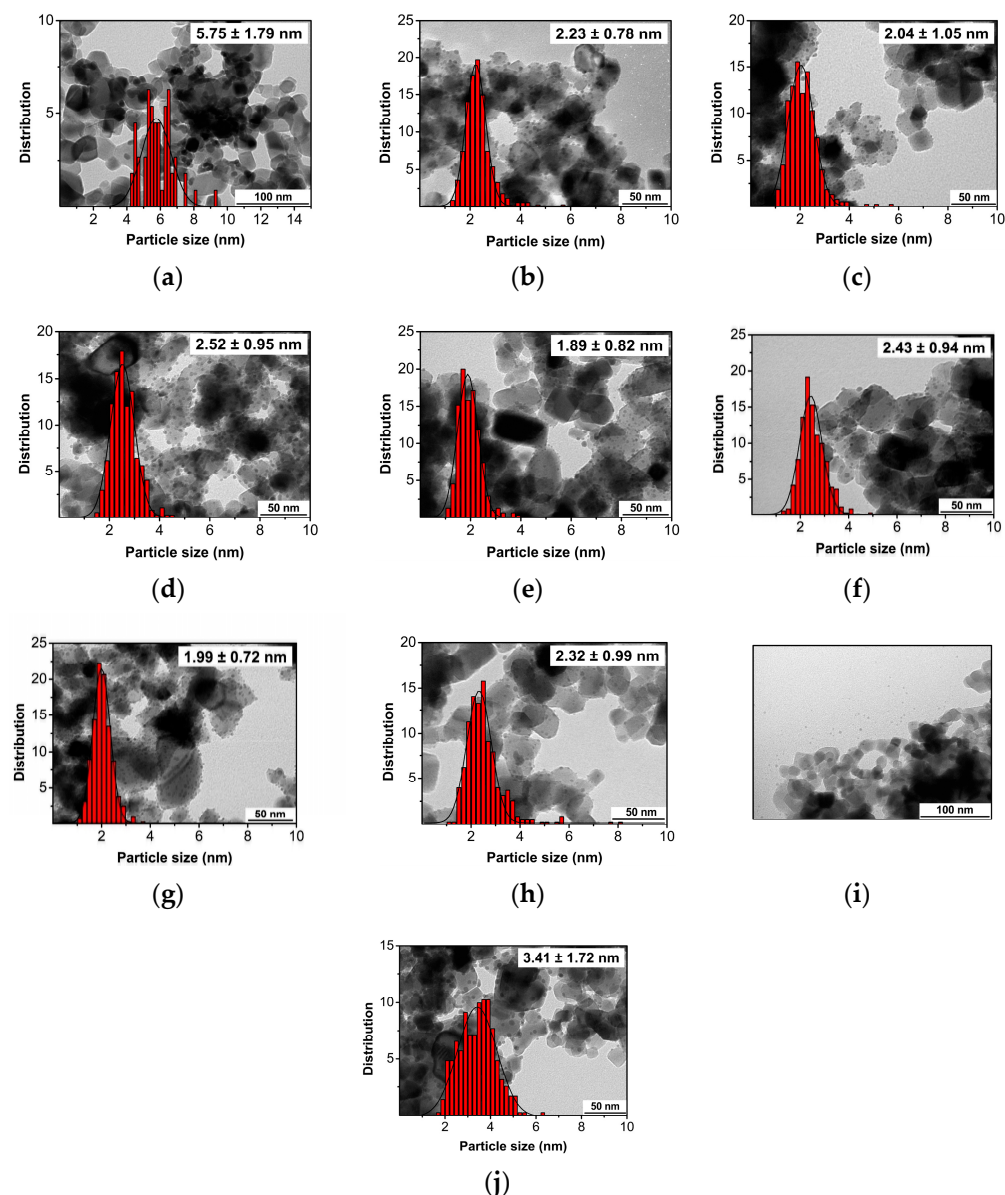


Figure 2. TEM images and size distributions of Pd NPs synthesized over modified TiO₂ supports. Deposition of TESs and PAs modifiers over previously synthesized Pd-PPh₃ supported over TiO₂. 1 (a), 2 (b), 3a (c), 3b (d), 4 (e), 5 (f), 6a (g), 6b (h), 7 (i), and 8 (j).

When the PA containing an alkylic chain was used for the modification of the support (Figure 2i), large Pd agglomerations were observed, and nanoparticles were detected out of the support. This indicates that using this modified support, the NP stabilization was not efficient. When the PA containing an amine group was used as the support modifier (Figure 2j), the sizes of the resulting Pd NPs were 3.41 nm, while similar Pd contents were obtained by ICP (ca. 3.3 wt%) (Table S3). Both samples revealed Pd NPs with broad distributions. The material 8, containing TiO₂ modified by PAs, was analyzed by HR-TEM (Figure S13). Small agglomerations were observed by HR-HAADF STEM. The presence of phosphorus was detected over the support and over the Pd NPs due to the presence of NH₂-PA and PPh₃.

These results therefore indicated that when organosilanes (TESs) were used to modify TiO₂, the NP stabilization was efficient, resulting in smaller Pd NPs with narrower distributions than for PA-modified supports. However, in terms of Pd loading, no relevant differences were observed. The presence of functional groups in the TESs modifiers also affected the NP stabilization since the materials containing an organosilane with a simple

alkyl chain provided larger Pd NPs with broader distribution than with TESs containing either an amine function or an imidazolium group.

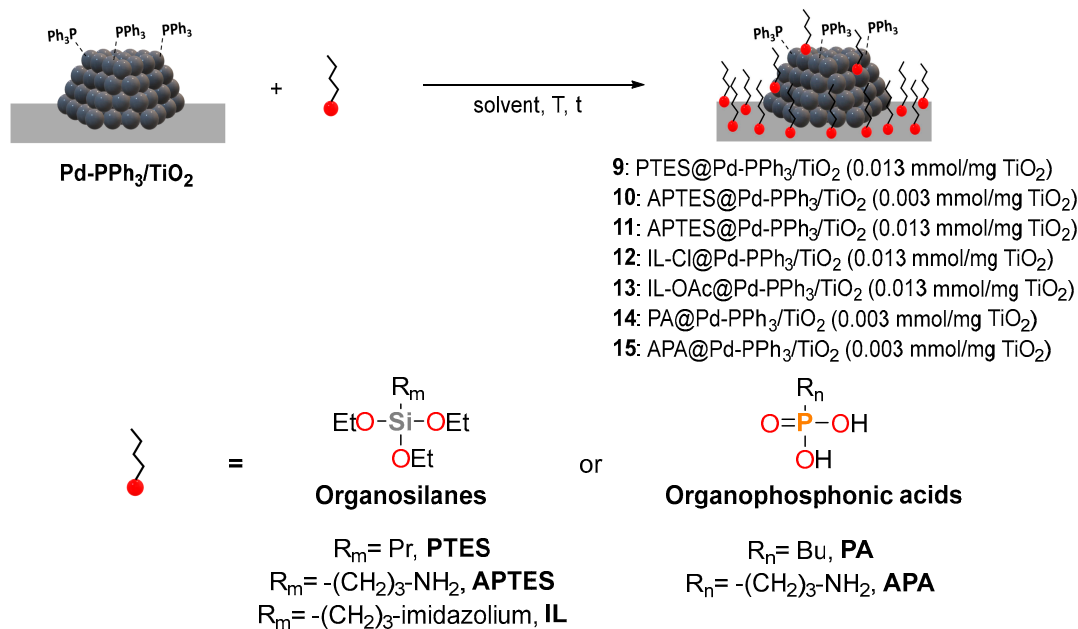
Moreover, when the synthesis was performed using the support with a higher concentration of APTES, smaller nanoparticles were obtained. The same effect was observed when IL-containing modifiers were used.

XPS analysis was also performed for some of the **Pd-PPh₃/mod@TiO₂** 1–8 catalysts (Table S4 and Figures S14–S16) to obtain the surface composition data, chemical state, and electronic state of different elements present in these catalysts. The data obtained were compared with those of the unmodified **Pd-PPh₃/TiO₂** catalyst. All the spectra were referenced using the C1s signal and set at 285.0 eV. The presence of Si2p, N1s, and P2p for **4** catalyst and N1s and P2p for **8** was detected. For Pd3d, no significant differences were observed with the unmodified **Pd-PPh₃/TiO₂** catalyst (335.0 eV). For all the samples, the relative amount of Pd^{δ+} also revealed similar (ca. 10%).

To conclude, the synthesis and characterization of the series of catalysts 1–8 based on PPh₃-capped Pd NPs were carried out using modified supports. When organosilanes were employed to modify the support, smaller Pd NPs were obtained than when the supports were modified with organophosphonic acids. The presence of the -NH₂ group in organosilanes and organophosphonic acids influences the structure/composition of the materials since in the absence of the -NH₂ group, large NPs as well as unsupported NPs and agglomerations were observed.

2.2. Deposition of Modifier over TiO₂-Supported PPh₃-Capped Pd NPs

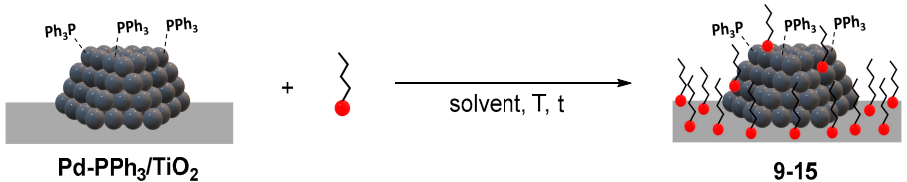
A new series of catalysts was synthesized by deposition of TESs and PAs modifiers over the previously synthesized **Pd-PPh₃/TiO₂** material (Scheme 4). The newly prepared systems were characterized by TEM and ICP, and FT-IR, TGA, HR-TEM, and XPS analyses were also performed for representative examples.



Scheme 4. Deposition of TESs and PAs modifiers over previously synthesized Pd-PPh₃ supported over TiO₂.

PTES or APTES was reacted with the previously synthesized **Pd-PPh₃/TiO₂** either at r.t. overnight in a mixture of 95% EtOH, 5% H₂O, or at 120 °C during 4 h using EtOH as solvent. At the end of the reaction, the samples were centrifugated, washed with milli-Q H₂O and EtOH, and dried overnight at 100 °C.

The samples were initially analyzed by TEM (Figure S17) and ICP, and the data are summarized in Table 1.

Table 1. Characterization data for the deposition of TESs and PAs over the previously synthesized Pd-PPh₃/TiO₂ system ¹.


Entry	System	Size (nm) ²	Pd wt% ³	P wt% ³
1	9	2.65 ± 0.80	3.38	-
2	10	2.69 ± 0.92	3.04	0.21
3	11	1.86 ± 0.69	2.57	-
4	12	2.38 ± 0.95	1.81	-
5	13	1.87 ± 0.61	2.98	-
6 ⁴	14	4.45 ± 1.68	3.10	0.82
7 ⁵	15	3.00 ± 1.14	3.15	-

¹ Synthesis conditions: Pd-PPh₃/TiO₂ previously synthesized was added to a solution of TESs (for determined mmol TESs/mg Pd-PPh₃/TiO₂ ratio) on mixture EtOH:milli-Q H₂O (95:5, v/v), and it was left to react at r.t. overnight. ² Determined by TEM. ³ Determined by ICP. ⁴ Pd-PPh₃/TiO₂ system was added to a solution of PA on THF, and it was left to react r.t. overnight. ⁵ Pd-PPh₃/TiO₂ system was added to a solution of APA on milli-Q H₂O, and it was left to react r.t. overnight.

As described previously, the Pd NPs in the Pd-PPh₃/TiO₂ catalyst exhibited a mean size of 2.37 ± 0.19 nm [80]. When the catalyst was modified by deposition of PTES (Entry 1), the size of Pd NPs slightly increased to 2.65 ± 0.80 nm, and a Pd content of 3.38 wt% was measured by ICP. When APTES was used as the modifier, the mean size of the NPs varied from ca. 1.9 (Entry 3) to 2.7 nm (Entry 2), indicating little effect of the treatment on the Pd NPs. However, relevant decreases in Pd content were observed, indicating that the deposition of modifiers containing an amine group could induce the leaching of Pd from the previously synthesized material. The presence of P (from PPh₃) and Si (from the organosilane) was confirmed by ICP.

When modifiers containing imidazolium groups in the alkyl chain were tested, the NPs mean diameters were between ca. 1.9 (Entry 5) and 2.4 nm (Entry 4), with distributions narrower than 1 nm. However, the Pd content was lower than expected. Surprisingly, when PAs were deposited over Pd-PPh₃/TiO₂, larger NP sizes were observed, as mean diameters of 4.45 ± 1.68 nm (Entry 6) and 3.00 ± 1.14 nm (Entry 7) were measured when PA and APA were employed, respectively. This therefore indicated that the deposition of PAs over Pd-PPh₃/TiO₂ caused a restructuring of the Pd NPs. In contrast, for these catalysts, the Pd content was almost the same as that in the original material, thus suggesting that the reaction of the previously synthesized material with PAs does not induce Pd leaching but could produce some restructuring, such as Ostwald's ripening.

Comparing the NP sizes obtained via the two approaches described in this work, modification over the pre-synthesized Pd-PPh₃/TiO₂ NPs (Table S3) yielded smaller Pd NPs and narrower distributions than when the TiO₂ support was modified in the first step (Table 1). However, lower Pd contents were obtained.

FT-IR and TGA analyses were also performed on **11** (Figure S18). Comparing the FT-IR spectra of this sample with that of TiO₂-3 (Figure S18a) (same concentrations and conditions), the same IR signals were detected. However, the TGA analysis revealed a greater amount of organic material at the surface of TiO₂-3 (Figure S18b).

From HR-TEM analysis of **11** (Figure 3 and Figure S20a), a thin layer was detected at the surface of the material. A similar observation was reported by Liu et al. using APTES as the modifier [56]. This layer was ca. 2 nm thick and wrapped both support and Pd particles. EDS mapping (Figure S20c) revealed the Si-based nature of this layer at the surface of both TiO₂ and Pd NPs. Therefore, this evidenced a structural difference for the materials obtained by this approach when compared with those synthesized by reverse deposition.

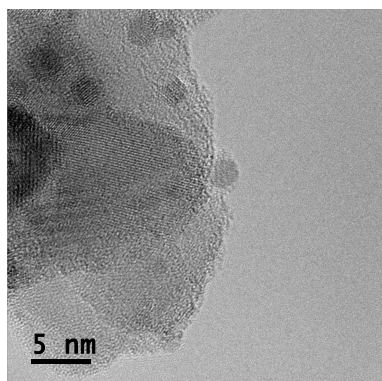


Figure 3. HR-TEM image of the catalyst **11**.

When HR-TEM analysis of **12** was performed (Figure S21), agglomerations were detected in some regions of the support (Figure S21a,b). Microanalysis also confirmed the presence of P originating from the PPh₃ ligands.

XPS was also employed for the analysis of some of these catalysts (Figures S24–S26). The data obtained were compared with those of the unmodified Pd-PPh₃/TiO₂ catalyst. All the spectra were referenced using the C1s signal and set at 285.0 eV. The presence of Si2p, N1s, and P2p for **11** catalyst and N1s and P2p for **15** was detected. The Pd spectra were studied with more detail (Figure S26b). When a P-based modifier was used (**15**), no significant differences with the unmodified catalyst were observed. However, for the sample containing the Si-based modifiers, the BEs observed were higher. For **11**, a difference of 1 eV was observed (336.0 eV) with the reference catalyst, which could be due to the interaction with the amine functional group from APTES, as previously reported by Kim et al. [82]. They also observed an increase of BE for Pd when APTES was used on the synthesis of Pd NPs over CNTs, and this difference was attributed due to the interaction of Pd with amine functional groups and to the particle size (1.85 nm). A combination of interaction of amine and small size could produce the BE observed for **11**.

The relative amount of Pd^{δ+} also revealed differences in samples (Table S6). In unmodified Pd-PPh₃/TiO₂, a value of 12.5% was measured. When the aminophosphonic acid was used in the synthesis of **15**, the proportion of Pd^{δ+} was 21.9%. These values remained similar to that of the reference Pd-PPh₃/TiO₂ catalyst. However, a value as high as 64% was obtained for **11** that was attributed to the oxidation of the samples during manipulations.

To conclude, these new catalysts were obtained by deposition of organosilane and organophosphonic acid modifiers over previously synthesized Pd NPs supported on TiO₂. When organosilanes were employed as modifiers, smaller Pd NPs were obtained compared with those modified by organophosphonic acids. Using APTES at different concentrations, the use of a greater amount of APTES led to lower Pd contents, which was attributed to Pd leaching.

2.3. Hydrogenation of CO₂ into Formates Using Modified Catalysts

First, a screening was performed to evaluate the effect of the different modifications carried out on catalysts. These tests were performed at 80 °C using 36 bar of CO₂/H₂ (1:1) pressure during 15 h in the presence of KHCO₃ as a base and using water as solvent. The results obtained using the Pd-PPh₃/modifier@TiO₂ 1–8 and modifier@Pd-PPh₃@TiO₂ 9–15 catalysts are summarized in Tables 2 and 3.

2.3.1. Hydrogenation of CO₂ into Formates Using Catalysts Formed by Deposition of Pd NPs over Modified TiO₂ Supports

In Table 2, the results obtained with systems 1–8 are displayed and compared with those provided by the unmodified Pd-PPh₃/TiO₂ catalyst (TON of 881, Entry 1) under the same conditions [80]. When **2** was used as catalyst, a TON of 1057 was reached (Entry 3),

whereas using material **8**, modified by organophosphonic acid (Entry 11), a decrease in activity was observed, and the lowest TON value of the series was measured (694). These results therefore indicated that when the catalyst is formed by deposition of the Pd NPs over the modified support, the nature of the modifier affects the catalyst activity.

Table 2. Catalytic activity of Pd-PPh₃/modifier@TiO₂ 1–8 with different anchor atoms for CO₂ hydrogenation to formate¹.

$\text{CO}_2 + \text{H}_2 \xrightarrow[\text{4 M KHCO}_3, \text{ 5 ml milli-Q H}_2\text{O}]{\text{1-8}} \text{HCOOK}$ 36 bar (1:1), 80 °C, 15 h		
Entry	Catalyst	TON ²
1	Pd-PPh ₃ /TiO ₂	881
2	1	588
3	2	1057
4	3a	868
5 ³	3b	917
6	4	1043
7	5	1030
8	6a	776
9 ³	6b	826
10	7	635
11	8	694

¹ Reaction conditions: 20 mg of catalyst, 4 M KHCO₃, 5 mL milli-Q H₂O, 80 °C, pTotal = 36 bar, p(CO₂) = p(H₂), and 15 h. ² TON = mmol formate/mmol total of Pd, calculated by NMR using 1,4-dioxane as internal standard.

³ In absence of PPh₃.

Next, the effect of the reaction conditions used for the support modification using APTES was investigated. The results obtained show three distinct effects compared with the unmodified catalyst (Entry 1). When low concentrations of APTES (0.01 M and 0.003 mmol/mg TiO₂) were used to modify the support, a positive effect on the activity of the resulting catalyst **2** was observed (Entry 3). When the concentration of APTES was increased up to 0.1 M (up to 0.013 mmol/mg TiO₂) (catalyst **3a**, Entry 4), the TON obtained was similar to that obtained with the unmodified catalyst (868), suggesting that the excess of APTES “cancelled out” the positive effect observed at lower concentrations. These results are in contrast with those reported by Mori et al. [58] using a phenylamine containing organosilane to modify SiO₂ since they observed an increase in catalytic activity when the amount of phenylamine was increased.

Next, the effect of the functional group at the end of the alkyl chain of the modifier was evaluated. For the catalysts formed by modifications with organosilanes, the presence of a functional group (either NH₂ or imidazolium group) was clearly beneficial to the catalyst activity since an increase in TON was observed from 588 (for PTES, Entry 2) to ca. 850 for APTES and IL-OAc-modified catalysts (Entries 4 and 8). A similar effect was observed for PAs-modified catalysts (Entry 10 vs. 11), although to a lesser extent (635 vs. 694).

For the Pd NPs over TiO₂ previously modified by organosilanes containing an IL functionality, the highest TON was obtained with the catalyst **5** (1030, Entry 7).

Based on previous results using organosilane modifiers (Table 2), the concentration could be the parameter responsible for this difference. This was confirmed by the results obtained with the catalysts **5** and **6a**, which only differ in the concentrations used during their support synthesis (Entry 7 vs. Entry 8). Indeed, the catalyst **5** containing the support modified at the lower concentration provided a TON of 1030, while when **6a** was used, a TON of 776 was obtained. These results are therefore in agreement with the trend previously observed.

The presence of the PPh₃ ligand during the synthesis of the Pd NPs over supports modified with APTES and IL-OAc was evaluated (Table 2). In both cases, slightly higher TON values were obtained in the absence of PPh₃ (Entry 4 vs. Entry 5 and Entry 8 vs.

Entry 9). When **3a** was used, a TON of 868 was obtained (Entry 4), while in the system without PPh₃, **3b** provided a TON of 917 (Entry 5). IL-OAc, **6a**, which was synthesized in the presence of PPh₃, reached a TON of 776 (Entry 8), while its analogue without PPh₃, **6b**, yielded a TON of 826 (Entry 9).

These catalytic results therefore show that the modification of the TiO₂ support by organosilanes provided a beneficial effect compared with the catalyst containing unmodified TiO₂ or TiO₂ modified by organophosphonic acids. Moreover, the modifier concentration is a key parameter during the support modification, and lower values provide catalysts with higher activities. The presence of a functional group (either NH₂ or imidazolium) in the modifiers also improved the activity of the catalysts compared with those containing a simple alkyl chain.

2.3.2. Hydrogenation of CO₂ into Formates Using Catalysts Formed by Modifications of Pre-Synthesized Pd-PPh₃/TiO₂

The catalysts synthesized by the deposition of the modifier over previously synthesized Pd-PPh₃/TiO₂ were evaluated in the hydrogenation of CO₂ into formate (Table 3).

Table 3. Catalytic activity of **modifier@Pd-PPh₃/TiO₂** 9–15 with different anchor atoms for CO₂ hydrogenation to formate¹.

$\text{CO}_2 + \text{H}_2 \xrightarrow[\text{36 bar (1:1), 80 }^\circ\text{C, 15 h}]{\text{9-15, 4 M KHCO}_3, \text{ 5 ml milli-Q H}_2\text{O}} \text{HCOOK}$		
Entry	System	TON ²
1	Pd-PPh ₃ /TiO ₂	881
2	9	862
3	10	581
4	11	992
5	12	388
6	13	551
7	14	912
8	15	844

¹ Reaction conditions: 20 mg of catalyst, 4 M KHCO₃, 5 mL milli-Q H₂O, 80 °C, p_{Total} = 36 bar, p(CO₂) = p(H₂), and 15 h. ² TON = mmol formate/mmol total of Pd, calculated by NMR using 1,4-dioxane as internal standard.

When the results obtained by the deposition of organosilane and organophosphonic acid under the same conditions (same concentration, mmol modifier/mg TiO₂ ratio, and amine substituent on the organosilane and organophosphonic acid) were compared, the system containing a Si as anchoring atom, **10**, provided a TON of 581 (Entry 3), whereas when APA was used as modifier, in **15**, a TON of 844 was reached (Entry 8).

As the unmodified catalyst provided a TON of 881, it was concluded that the deposition of the organosilane over the pre-synthesized catalyst had a detrimental effect on the CO₂ hydrogenation, while the deposition of PA had no significant effect. These results are in contrast with those obtained using the catalyst where Pd NPs were deposited over the modified support, and they highlight the importance of the synthetic strategy when such catalysts are modified with organic molecules.

The results obtained for hydrogenation of CO₂ to formate using catalysts formed by the deposition of APTES at different concentrations are also summarized in Table 3. As previously mentioned, the system **10** obtained at low concentration (0.01 M of APTES; 0.003 mmol/mg TiO₂), and the TON obtained was 581. However, when the same modifier was deposited using a 0.13 M solution, the resulting catalyst **11** provided much higher activity with a TON of 992 (Entry 4).

The performance of catalysts modified by organosilanes containing a propyl, a propylamine, or a propyl-imidazolium groups and those modified by PAs containing a butyl and a propylamine substituent was also evaluated (Table 3). Interestingly, all these catalysts

exhibited activities similar to that of the unmodified catalyst, except that modified by an organosilane containing an imidazolium function. It is noteworthy that, as described in the previous section, the catalyst **11** showed a slight positive effect compared to the reference catalyst (Entry 4 vs. Entry 1). The results described here are in clear contrast with those obtained when the support was first modified prior to the deposition of Pd NPs, for which the presence of a functional group (either amine or imidazolium) in the modifier clearly improved the performance of the resulting catalysts. This might be due to the beneficial effect of this group in the anchoring of the NPs when present at the support surface prior to the NP deposition, while such a group does not influence the catalytic activity when deposited after NP formation. This thus suggests that the presence of this group does not influence the catalysis but only the preparation of the catalyst.

The catalytic performances of the catalysts **12** and **13**, modified by ionic liquid-containing modifiers with distinct anions, are summarized Table 3. The two catalysts tested provided lower TONs (388 and 551, Entries 5 and 6, respectively) than the unmodified catalyst, indicating that the deposition of IL-containing organosilanes over the Pd NPs was detrimental to the catalytic performance of the **Pd-PPh₃/TiO₂** material.

These catalytic results therefore show that the deposition of organosilane and organophosphonic acid modifiers over previously synthesized Pd NPs supported on TiO₂ was not beneficial, in most cases, to the activity of the resulting catalysts.

The TON values obtained using the catalysts described here are among the highest reported for Pd-based catalysts (range ca. 800–1200) [42,58,83,84].

2.3.3. Reusability Tests

After evaluating the activity of the newly synthesized catalysts, recyclability tests were performed using the most active systems. During these experiments, the catalysts were recovered by filtration over a Nylon membrane after each cycle, washed several times with milli-Q H₂O, and dried under vacuum for several hours prior to their reuse. All the experiments described in the manuscript were carried out at least twice to confirm the reproducibility of the data.

Initially, the catalysts **2**, **3b**, **4**, and **8** were employed to evaluate the effect of the modifiers on the reusability of the materials performing the hydrogenation reactions at 80 °C. The results obtained are summarized in Figure 4. In all cases, a strong decrease in activity was observed after two cycles. However, the catalysts **2** and **3b** containing the support previously modified by APTES suffered a minimal loss of activity during the first cycle and a large decrease during the second cycle. In contrast, the catalysts **4** and **8** containing the support modified by NH₂-PA and an organosilane containing an imidazolium group suffered a large loss of activity during the first recycling but maintained their activity during the second recycling. After the third recycling, a new drop in activity for these catalysts was observed. TEM analysis of the spent catalysts revealed large agglomerations in all samples, while no dramatic changes in mean size were measured on non-agglomerated Pd NPs (Figures S40, S41, S43 and S44).

Next, recyclability experiments were performed using the catalysts **11**, **12**, **14**, and **15** under the same conditions (Figure 5). It was found that **11** was the most active system of this series, with an initial TON of 904. This catalyst provided a TON of 724 after the first recycling, 662 after the second recycling, and 524 after the third recycling.

For the catalysts in which deposition of an organophosphonic acid was performed over the previously synthesized **Pd-PPh₃/TiO₂**, distinct behaviors were observed depending on the functional groups contained in the modifiers. For **15** containing a PA with an amine function, a drastic decrease in activity was observed during the first recycling, with a drop of TON value from 873 to 332. No relevant decrease in activity was observed during the second recycling, while a drop of TON to 201 was measured for the third recycling. In contrast, when the catalyst contained a PA modifier with a butyl chain **14**, the activity loss during the first recycling was less pronounced (from a TON of 827 to 723), while a sudden drop to 369 was observed during the second recycling. For the catalyst **12** modified by

an organosilane containing an imidazolium group, much lower activities were measured (TONs of 405 initially and 209 after three runs).

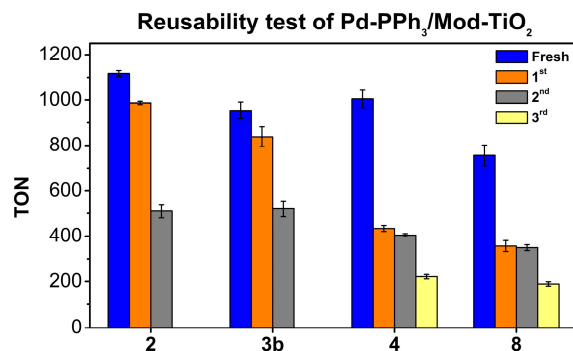


Figure 4. Recycling experiments with catalysts **2**, **3b**, **4**, and **8** in CO₂ hydrogenation to formate. Conditions: 20 mg of catalyst, 4 M KHCO₃, 5 mL milli-Q H₂O, p_{Total} = 36 bar, p(CO₂) = p(H₂), 80 °C, and 15 h. TON = mmol formate/mmol total of Pd, calculated by NMR using 1,4-dioxane as internal standard.

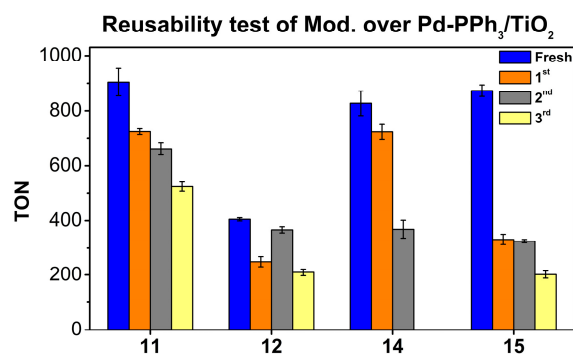


Figure 5. Recycling experiments with the systems **11**, **12**, **14**, and **15** in the hydrogenation of CO₂ to formate. Conditions: 20 mg of catalyst, 4 M KHCO₃, 5 mL milli-Q H₂O, p_{Total} = 36 bar, p(CO₂) = p(H₂), 80 °C, and 15 h. TON = mmol formate/mmol total of Pd, calculated by NMR using 1,4-dioxane as internal standard.

TEM analysis of the spent catalysts after two recyclings (Figure S45) revealed that the mean sizes of the Pd NPs in these materials was in all cases in the range 3.5–4 nm (Table S19), and different degrees of agglomeration were observed. In the case of catalyst **12**, for which an increase in Pd NPs mean size from 2.4 nm to ca. 4 nm was observed, the presence of agglomerations was pronounced. For the catalysts modified with PAs **14** and **15**, no large variation in size was observed, but large agglomerations were detected.

These recycling experiments therefore show that the synthetic procedure used for the modification of the Pd-PPh₃/TiO₂ catalyst affects the reusability of these materials in the CO₂ hydrogenation into formate. Indeed, the catalysts formed by modification of the support prior to Pd NP deposition suffer a rapid decrease in activity during their recycling and reuse in spite of the initial beneficial effect. In contrast, some of the materials where the modifiers were deposited over the previously anchored Pd NPs onto TiO₂ show a much more gradual decrease in activity and reached a TON > 500 after the third recycling. To evidence the improvement in reusability obtained by catalyst modification in this work, the TON values obtained with the unmodified catalyst Pd-PPh₃/TiO₂ during the recycling experiments are compared with those of **11** in Figure 6. Despite a superior initial activity of the unmodified catalyst, both materials exhibited similar TON values after the first recycling and in the second and third recyclings, and the modified catalyst clearly showed a better performance.

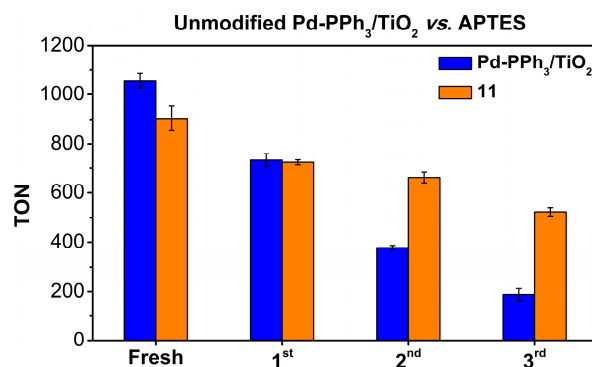


Figure 6. Comparison of recycling experiments with **11** and **Pd-PPh₃/TiO₂** for CO₂ hydrogenation to formate. Conditions: 20 mg of catalysts, 4 M KHCO₃, 5 mL milli-Q H₂O, p_{Total} = 36 bar, p(CO₂) = p(H₂), and 15 h. Temperatures employed for **11** and **Pd-PPh₃/TiO₂** were 80 and 60 °C, respectively. TON = mmol formate/mmol total of Pd, calculated by NMR using 1,4-dioxane as internal standard.

Important differences were observed by TEM analyses of the spent catalysts since for **11**, an increasing of size from 1.86 ± 0.69 nm to 3.53 ± 1.23 nm was measured after two cycles, but only a few agglomerations were observed. In contrast, the Pd NPs in **Pd-PPh₃/TiO₂** were largely agglomerated after the recyclings and exhibited a mean size of ca. 5 nm. These results suggest that the presence of APTES provided additional stabilization and limited the degree of agglomerations of the Pd NPs. This is in agreement with the previously reported results where modifications of the heterogeneous catalyst by APTES improved the stability of the catalysts and hence their recovery [53,54,56,58,59].

3. Materials and Methods

Pd(dba)₂, PPh₃, TiO₂ (Titanium (IV) oxide nanopowder, 21 nm primary particle size (TEM), $\geq 99.5\%$ trace metals basis, rutile–anatase mixture, specific surface area 35–65 m²/g), and the rest of compounds employed for modification were purchased from Sigma-Aldrich (St. Louis, MO, USA) and used without any further purification. All solvents were dried from a solvent purification system (SPS) and deoxygenated. Tetrahydrofuran was further dried by refluxing in the presence of sodium/acetophenone. Milli-Q water purchased from Merck (Madrid, Spain) was employed in catalytic experiments. Any other solvent or reagent employed was reagent-grade. Hydrogen (5.0) was purchased from Carbueros Metálicos (Barcelona, Spain), and CO₂ (5.3) was purchased from Abelló Linde (Valencia, Spain). All the synthesis were performed using Schlenk techniques under argon and glovebox using nitrogen as the inert gas. The synthesis of nanoparticles were carried in Fischer–Porter bottles, and catalytic tests were performed in the stainless-steel high-pressure reactor Hel CAT-7 (7 × 10 mL). Characterization techniques that were employed included TEM, HR-TEM, ESEM, FESEM, ICP-OES, TGA, NMR, FT-IR, and XPS. All details and corresponding figures can be found in the Supporting Information.

3.1. Modification of TiO₂ with *n*-Propyltriethoxysilane (PTES) and (3-Aminopropyl)triethoxysilane (APTES)

In a general synthesis of **TiO₂-1-3**, a solution (mixture EtOH:milli-Q H₂O 95:5 *v/v*) of the accorded concentration of PTES or APTES was prepared in a Schlenk (under Ar). Then, the corresponding amount of TiO₂ (mmol (A)PTES/mg TiO₂) (Table S1) was added to the solution under vigorous stirring. The reaction was stirred at room temperature overnight. Then, the mixture was centrifuged. The supernatant was removed, and the solid was washed several times with milli-Q H₂O and EtOH and was dried at 80 °C under vacuum for several hours.

3.2. Modification of TiO₂ with Ionic Liquids (ILs)

First, synthesis of the ILs was performed according to the literature with some variations [75,85–89]. The synthesis of **TiO₂-4** was performed according to reported procedures [86]. A suspension of 2 g of TiO₂ in 80 mL of milli-Q H₂O was added to a previously prepared solution of 659.08 mg (1.8 mmol) of IL-Cl in 2 mL of milli-Q H₂O. The mixture was stirred at 80 °C for 12 h (Table S1). After reaction, the mixture was centrifuged and washed twice with milli-Q and once with EtOH. After that, it was dried under vacuum at 60 °C.

For the ILs with AcO[−] (**TiO₂-5** and **TiO₂-6**) as anion, TiO₂ was added to a solution of IL-OAc (mixture EtOH:milli-Q H₂O 95:5 *v/v*), and the mixture was heated at 80 °C overnight (Table S1). The product was washed with EtOH several times and dried under vacuum at 60 °C.

3.3. Modification of TiO₂ with Phosphonic Acids (PAs)

The modification of TiO₂ with PAs (**TiO₂-7** and **TiO₂-8**) was performed according to the literature procedures with some variations [90–92] (Table S1). Solutions contained 83.35 μmol of modifier per each square meter of TiO₂ nanopowder, which corresponded approximately to a 10-fold excess in respect to building a monolayer on the surface of the support.

A solution of 10 mM of 3-aminopropylphosphonic acid (APA) (**TiO₂-8**) (1.46 mmol, 202.84 mg) in 146 mL of milli-Q H₂O was prepared. Then, 0.5 g of TiO₂ was added, and the mixture was stirred at r.t. overnight. After this time, the suspension was centrifuged and washed with abundant milli-Q water, EtOH, and acetone. The solid was dried at 120 °C in an oven. It is necessary to produce condensation reactions to yield strong bonds between PAs and metal oxide [39]. So, in this case, after the reaction, the solid was separated by centrifugation, the solvent was removed, and the solid was placed into an oven at 100 °C overnight. After that, the solid was aged in a Quartz furnace at 120 °C under air flow during 6 h. Then, it was washed with abundant milli-Q water and centrifuged every time (5 times). The solid was dried overnight at 100 °C. When butylphosphonic acid was employed (PA) (**TiO₂-7**), the synthesis was performed under the same conditions (Table S1). The only difference was that THF was used as the reaction media and for washing and centrifugation.

3.4. Synthesis of Pd NPs with PPh₃ as Ligand over Different Modified TiO₂ Supports through Organometallic Approach (1–8)

The catalysts were prepared following a previously reported methodology [80] to obtain a 4 wt% theoretical content of Pd over TiO₂. In a common experiment, the metal precursor (Pd(dba)₂), 0.2 eq. of stabilizer (PPh₃), and modified TiO₂ were weighted in the glove box and charged in a Fischer–Porter bottle. Then, solvent (THF) was added; the Fischer–Porter was closed and purged with hydrogen several times and then charged with 3 bar of H₂. The mixture was then heated at 60 °C and stirred at 700 rpm overnight. After the reaction, the mixture was cooled to room temperature and degassed. Samples for TEM analysis were prepared by the deposition of several drops of the reaction crude onto a copper grid. The rest of the reaction crude was concentrated and washed several times with abundant hexane. The catalyst was dried under vacuum during several hours.

3.5. Deposition of Modifier over Previously Synthesized Pd-PPh₃/TiO₂ Systems (9–15)

PTES and APTES (9–11): A specified concentration of PTES or APTES (and determined mmol (A)PTES/mg: Pd-PPh₃/TiO₂ ratio) and Pd-PPh₃/TiO₂ that was previously synthesized were mixed (Table S5). At r.t., the synthesis was carried out overnight in Schlenk using a mixture of 95% EtOH and 5% milli-Q H₂O, while reactions at 120 °C reaction temperature were performed in an autoclave during 4 h using EtOH as solvent. In both cases, samples were dried overnight in an oven at 105 °C and stored inside the glove box.

ILs (12–13): A mixture of a specified concentration of IL–anion and the previously synthesized **Pd-PPh₃/TiO₂** system was prepared at r.t. using a mixture of 95% EtOH and 5% milli-Q H₂O, overnight (Table S5).

PAs (14–15): A mixture of a specified concentration of PAs and the previously synthesized **Pd-PPh₃/TiO₂** system was prepared at r.t. using milli-Q H₂O as solvent (for synthesis with APA) or THF (for synthesis with PA), overnight (Table S5).

3.6. Catalytic Experiments for CO₂ Reduction to Formate

The stainless-steel high-pressure reactor HEL CAT-7 (7 × 10 mL) was charged with TiO₂-supported palladium nanoparticles (20 mg), 20 mg of 1,4-dioxane, and 5 mL of a 4 M base solution employing milli-Q water. The reactor was first flushed with 3 cycles of hydrogen to remove the air. Then, the reactor was charged with 10 bar of H₂ and heated at 40 °C under stirring for twenty minutes. At this point, the reactor was depressurized, purged several times with CO₂, and charged with 18 bar of CO₂ and left under stirring for 20 min. Then, the reactor was charged with 18 bar of H₂ (1:1, CO₂:H₂) and heated to reach the temperature under 600 rpm of stirring. The experiment was left 15 h, and after this time, the reactor was allowed to cool in an ice bath. When the reactor was cooled, it was depressurized and opened. A small amount of the sample was centrifuged, and 100 µL of supernatant was analyzed by NMR using D₂O as the deuterated solvent.

3.7. Recycling Experiments

After every catalytic experiment, the mixture was filtered through a Nylon membrane. The solid was washed several times with abundant milli-Q H₂O and dried under vacuum for several hours. At this point, the solid was reused in an identical catalytic experiment.

4. Conclusions

A series of supported Pd NPs-based materials were successfully synthesized using modifiers of different natures (organosilanes, ILs, and PAs) following two distinct approaches. The so-called reverse deposition approach requires in the first place to modify the TiO₂ support prior to Pd NPs deposition, while the second approach involves the modification of a pre-synthesized **Pd-PPh₃/TiO₂** by deposition of the modifier over its surface. The newly prepared materials, including the modified TiO₂ supports, were characterized by various techniques, such as TEM, HRTEM, EDS, FT-IR, TGA, ICP, etc.

These catalysts were tested in the hydrogenation of CO₂ to formate, and their performance was compared with those of the unmodified catalyst **Pd-PPh₃/TiO₂**. The modification of the TiO₂ support by organosilanes provided a beneficial effect in catalysis compared with the catalyst containing unmodified TiO₂ or TiO₂ modified by organophosphonic acids, and the modifier concentration is a key parameter during the support modification.

The presence of a functional group (either NH₂ or imidazolium) in the modifiers improved the activity of the catalysts. In contrast, the deposition of organosilane and organophosphonic acid modifiers over previously synthesized Pd NPs supported on TiO₂ was not beneficial, in most cases, to the activity of the catalyst.

The synthetic procedure used for the modification of the **Pd-PPh₃/TiO₂** catalyst also affected the reusability of these materials in the hydrogenation of CO₂ into formate, and when the modifiers were deposited over the previously anchored Pd NPs onto TiO₂, a more gradual decrease in activity was observed.

Supplementary Materials: The following supporting information can be downloaded at: <https://www.mdpi.com/article/10.3390/catal14080487/s1>. Synthetic procedures, technics data, TEM, XRD, XPS, EDX, HRTEM images, and results of catalysis experiment of hydrogenation of CO₂ under different conditions.

Author Contributions: Writing—original draft preparation, data curation, M.D.F.-M.; methodology, writing—review and editing, supervision, C.G. All authors have read and agreed to the published version of the manuscript.

Funding: This research was funded by the Spanish Ministerio de Ciencia e Innovación (CTQ2016-75016-R and PID2019-104427RB-I00) and the Generalitat de Catalunya (2017SGR1472 and 2021SGR00163) for financial support and the FPI grant (BES-2017-081305).

Data Availability Statement: The original contributions presented in the study are included in the article (and Supplementary Material), further inquiries can be directed to the corresponding authors.

Acknowledgments: The authors are grateful to the Spanish Ministerio de Ciencia e Innovación (CTQ2016-75016-R and PID2019-104427RB-I00) and the Generalitat de Catalunya (2017SGR1472) for financial support and the FPI grant (BES-2017-081305). Authors also thank the Servei of Recursos Científics i Tècnics of Universitat Rovira i Virgili for the analytical assistance and the Fundació Institut Català de Nanociència i Nanotecnologia (ICN2).

Conflicts of Interest: The authors declare no conflicts of interest.

References

1. Centi, G.; Perathoner, S. Opportunities and prospects in the chemical recycling of carbon dioxide to fuels. *Catal. Today* **2009**, *148*, 191–205. [[CrossRef](#)]
2. Centi, G.; Quadrelli, E.A.; Perathoner, S. Catalysis for CO₂ conversion: A key technology for rapid introduction of renewable energy in the value chain of chemical industries. *Energy Environ. Sci.* **2013**, *6*, 1711–1731. [[CrossRef](#)]
3. Dibenedetto, A.; Angelini, A.; Stufano, P. Use of carbon dioxide as feedstock for chemicals and fuels: Homogeneous and heterogeneous catalysis. *J. Chem. Technol. Biotechnol.* **2014**, *89*, 334–353. [[CrossRef](#)]
4. Koolen, C.D.; Oveisi, E.; Zhang, J.; Li, M.; Safonova, O.V.; Pedersen, J.K.; Rossmeisl, J.; Luo, W.; Züttel, A. Low-temperature non-equilibrium synthesis of anisotropic multimetallic nanosurface alloys for electrochemical CO₂ reduction. *Nat. Synth.* **2024**, *3*, 45–57. [[CrossRef](#)]
5. Raveendran, A.; Chandran, M.; Dhanusuraman, R. A comprehensive review on the electrochemical parameters and recent material development of electrochemical water splitting electrocatalysts. *RSC Adv.* **2023**, *13*, 3843–3876. [[CrossRef](#)] [[PubMed](#)]
6. Ohi, J. Hydrogen energy cycle: An overview. *J. Mater. Res.* **2005**, *20*, 3180–3187. [[CrossRef](#)]
7. Lee, J.H.; Ryu, J.; Kim, J.Y.; Nam, S.-W.; Han, J.H.; Lim, T.-H.; Gautam, S.; Chae, K.H.; Yoon, C.W. Carbon dioxide mediated, reversible chemical hydrogen storage using a Pd nanocatalyst supported on mesoporous graphitic carbon nitride. *J. Mater. Chem. A* **2014**, *2*, 9490–9495. [[CrossRef](#)]
8. Zhong, H.; Iguchi, M.; Chatterjee, M.; Ishizaka, T.; Kitta, M.; Xu, Q.; Kawanami, H. Interconversion between CO₂ and HCOOH under basic conditions catalyzed by PdAu nanoparticles supported by amine-functionalized reduced graphene oxide as a dual catalyst. *ACS Catal.* **2018**, *8*, 5355–5362. [[CrossRef](#)]
9. Park, H.; Lee, J.H.; Kim, E.H.; Kim, K.Y.; Choi, Y.H.; Youn, D.H.; Lee, J.S. A highly active and stable palladium catalyst on a g-C₃N₄ support for direct formic acid synthesis under neutral conditions. *Chem. Commun.* **2016**, *52*, 14302–14305. [[CrossRef](#)]
10. Shao, X.; Miao, X.; Yu, X.; Wang, W.; Ji, X. Efficient synthesis of highly dispersed ultrafine Pd nanoparticles on a porous organic polymer for hydrogenation of CO₂ to formate. *RSC Adv.* **2020**, *10*, 9414–9419. [[CrossRef](#)]
11. Su, J.; Lu, M.; Lin, H. High yield production of formate by hydrogenating CO₂ derived ammonium carbamate/carbonate at room temperature. *Green Chem.* **2015**, *17*, 2769–2773. [[CrossRef](#)]
12. Wang, W.-H.; Feng, X.; Bao, M. *Transformation of CO₂ to Formic Acid or Formate over Heterogeneous Catalysts*; Chapter 3; Springer: Berlin/Heidelberg, Germany, 2017; pp. 43–52, ISBN 978-981-10-3250-9.
13. Nakajima, K.; Tominaga, M.; Waseda, M.; Miura, H.; Shishido, T. Highly Efficient Supported Palladium–Gold Alloy Catalysts for Hydrogen Storage Based on Ammonium Bicarbonate/Formate Redox Cycle. *ACS Sustain. Chem. Eng.* **2019**, *7*, 6522–6530. [[CrossRef](#)]
14. Kuwahara, Y.; Fujie, Y.; Mihogi, T.; Yamashita, H. Hollow Mesoporous Organosilica Spheres Encapsulating PdAg Nanoparticles and Poly(Ethyleneimine) as Reusable Catalysts for CO₂ Hydrogenation to Formate. *ACS Catal.* **2020**, *10*, 6356–6366. [[CrossRef](#)]
15. Yang, G.; Kuwahara, Y.; Masuda, S.; Mori, K.; Louis, C.; Yamashita, H. PdAg nanoparticles and aminopolymer confined within mesoporous hollow carbon spheres as an efficient catalyst for hydrogenation of CO₂ to formate. *J. Mater. Chem. A* **2020**, *8*, 4437–4446. [[CrossRef](#)]
16. Mori, K.; Sano, T.; Kobayashi, H.; Yamashita, H. Surface Engineering of a Supported PdAg Catalyst for Hydrogenation of CO₂ to Formic Acid: Elucidating the Active Pd Atoms in Alloy Nanoparticles. *J. Am. Chem. Soc.* **2018**, *140*, 8902–8909. [[CrossRef](#)] [[PubMed](#)]
17. Nguyen, L.T.M.; Park, H.; Banu, M.; Kim, J.Y.; Youn, D.H.; Magesh, G.; Kim, W.Y.; Lee, J.S. Catalytic CO₂ hydrogenation to formic acid over carbon nanotube-graphene supported PdNi alloy catalysts. *RSC Adv.* **2015**, *5*, 105560–105566. [[CrossRef](#)]
18. Shao, X.; Xu, J.; Huang, Y.; Su, X.; Duan, H.; Wang, X.; Zhang, T. Pd@C₃N₄ nanocatalyst for highly efficient hydrogen storage system based on potassium bicarbonate/formate. *AIChE J.* **2016**, *62*, 2410–2418. [[CrossRef](#)]
19. Wan, K.T.; Davis, M.E. Design and synthesis of a heterogeneous asymmetric catalyst. *Nature* **1994**, *370*, 449–450. [[CrossRef](#)]
20. Shibasaki-Kitakawa, N.; Honda, H.; Kuribayashi, H.; Toda, T.; Fukumura, T.; Yonemoto, T. Biodiesel production using anionic ion-exchange resin as heterogeneous catalyst. *Bioresour. Technol.* **2007**, *98*, 416–421. [[CrossRef](#)] [[PubMed](#)]

21. Liu, R.; Jin, R.; An, J.; Zhao, Q.; Cheng, T.; Liu, G. Hollow-Shell-Structured Nanospheres: A Recoverable Heterogeneous Catalyst for Rhodium-Catalyzed Tandem Reduction/Lactonization of Ethyl 2-Acylarylcarboxylates to Chiral Phthalides. *Chem. Asian J.* **2014**, *9*, 1388–1394. [[CrossRef](#)]
22. Leng, Y.; Liu, J.; Jiang, P.; Wang, J. Organometallic-polyoxometalate hybrid based on V-Schiff base and phosphovanadomolybdate as a highly effective heterogenous catalyst for hydroxylation of benzene. *J. Chem. Eng.* **2014**, *239*, 1–7. [[CrossRef](#)]
23. Cong, P.; Doolen, R.D.; Fan, Q.; Giaquinta, D.M.; Guan, S.; McFarland, E.W.; Poojary, D.M.; Self, K.; Turner, H.W.; Weinberg, W.H. High-Throughput Synthesis and Screening of Combinatorial Heterogeneous Catalyst Libraries. *Angew. Chem. Int. Ed.* **1999**, *38*, 484–488. [[CrossRef](#)]
24. Uysal, B.; Oksal, B.S. New heterogeneous B(OEt)₃-MCM-41 catalyst for preparation of α,β -unsaturated alcohols. *Res. Chem. Intermed.* **2015**, *41*, 3893–3911. [[CrossRef](#)]
25. Yamaguchi, K.; Yoshida, C.; Uchida, S.; Mizuno, N. Peroxotungstate Immobilized on Ionic Liquid-Modified Silica as a Heterogeneous Epoxidation Catalyst with Hydrogen Peroxide. *J. Am. Chem. Soc.* **2005**, *127*, 530–531. [[CrossRef](#)] [[PubMed](#)]
26. Planeix, J.M.; Coustel, N.; Coq, B.; Brotons, V.; Kumbhar, P.S.; Dutartre, R.; Geneste, P.; Bernier, P.; Ajayan, P.M. Application of Carbon Nanotubes as Supports in Heterogeneous Catalysis. *J. Am. Chem. Soc.* **1994**, *116*, 7935–7936. [[CrossRef](#)]
27. Kent, P.D.; Mondloch, J.E.; Finke, R.G. A Four-Step Mechanism for the Formation of Supported-Nanoparticle Heterogeneous Catalysts in Contact with Solution: The Conversion of Ir(1,5-COD)Cl/ γ -Al₂O₃ to Ir(0)₋₁₇₀/ γ -Al₂O₃. *J. Am. Chem. Soc.* **2014**, *136*, 1930–1941. [[CrossRef](#)]
28. Dobrzeniecka, A.; Kulesza, P.J. Electrocatalytic Activity toward Oxygen Reduction of RuS_xN_y Catalysts Supported on Different Nanostructured Carbon Carriers. *ECS J. Solid State Sci. Technol.* **2013**, *2*, M61–M66. [[CrossRef](#)]
29. Astruc, D.; Lu, F.; Aranzas, J.R. Nanoparticles as Recyclable Catalysts: The Frontier between Homogeneous and Heterogeneous Catalysis. *Angew. Chem. Int. Ed.* **2005**, *44*, 7852–7872. [[CrossRef](#)]
30. Crudden, C.M.; Sateesh, M.; Lewis, R. Mercaptopropyl-Modified Mesoporous Silica: A Remarkable Support for the Preparation of a Reusable, Heterogeneous Palladium Catalyst for Coupling Reactions. *J. Am. Chem. Soc.* **2005**, *127*, 10045–10050. [[CrossRef](#)]
31. Lou, Y.; Xu, J.; Zhang, Y.; Pan, C.; Dong, Y.; Zhu, Y. Metal-support interaction for heterogeneous catalysis: From nanoparticles to single atoms. *Mater. Today Nano* **2020**, *12*, 100093. [[CrossRef](#)]
32. van Deelen, T.W.; Hernández Mejía, C.; de Jong, K.P. Control of metal-support interactions in heterogeneous catalysts to enhance activity and selectivity. *Nat. Catal.* **2019**, *2*, 955–970. [[CrossRef](#)]
33. Liu, L.; Corma, A. Metal Catalysts for Heterogeneous Catalysis: From Single Atoms to Nanoclusters and Nanoparticles. *Chem. Rev.* **2018**, *118*, 4981–5079. [[CrossRef](#)] [[PubMed](#)]
34. Sun, R.; Liao, Y.; Bai, S.-T.; Zheng, M.; Zhou, C.; Zhang, T.; Sels, B.F. Heterogeneous catalysts for CO₂ hydrogenation to formic acid/formate: From nanoscale to single atom. *Energy Environ. Sci.* **2021**, *14*, 1247–1285. [[CrossRef](#)]
35. Fan, F.; Zhang, J.; Ma, K.; Zhang, Y.; Hu, Y.-M.; Kong, L.; Jia, A.-P.; Zhang, Z.; Huang, W.; Lu, J.-Q. Ceria morphology-dependent Pd-CeO₂ interaction and catalysis in CO₂ hydrogenation into formate. *J. Catal.* **2021**, *397*, 116–127. [[CrossRef](#)]
36. Zhang, Z.; Zhang, L.; Hülsey, M.J.; Yan, N. Zirconia phase effect in Pd/ZrO₂ catalyzed CO₂ hydrogenation into formate. *Mol. Catal.* **2019**, *475*, 110461. [[CrossRef](#)]
37. Mori, K.; Yamashita, H. Design and Architecture of Nanostructured Heterogeneous Catalysts for CO₂ Hydrogenation to Formic Acid/Formate. In *CO₂ Hydrogenation Catalysis*, 1st ed.; Chapter 7; Himeda, Y., Ed.; Wiley-VCH GmbH: Weinheim, Germany, 2021; pp. 179–205.
38. Schoenbaum, C.A.; Schwartz, D.K.; Medlin, J.W. Controlling the Surface Environment of Heterogeneous Catalysts Using Self-Assembled Monolayers. *Acc. Chem. Res.* **2014**, *47*, 1438–1445. [[CrossRef](#)]
39. Jenkins, A.H.; Medlin, J.W. Controlling Heterogeneous Catalysis with Organic Monolayers on Metal Oxides. *Acc. Chem. Res.* **2021**, *54*, 4080–4090. [[CrossRef](#)] [[PubMed](#)]
40. Xu, L.; Cui, T.; Zhu, J.; Wang, X.; Ji, M. PdAg alloy nanoparticles immobilized on functionalized MIL-101-NH₂: Effect of organic amines on hydrogenation of carbon dioxide into formic acid. *New J. Chem.* **2021**, *45*, 6293–6300. [[CrossRef](#)]
41. Chen, B.; Dong, M.; Liu, S.; Xie, Z.; Yang, J.; Li, S.; Wang, Y.; Du, J.; Liu, H.; Han, B. CO₂ Hydrogenation to Formate Catalyzed by Ru Coordinated with a N,P-Containing Polymer. *ACS Catal.* **2020**, *10*, 8557–8566. [[CrossRef](#)]
42. Masuda, S.; Mori, K.; Futamura, Y.; Yamashita, H. PdAg Nanoparticles Supported on Functionalized Mesoporous Carbon: Promotional Effect of Surface Amine Groups in Reversible Hydrogen Delivery/Storage Mediated by Formic Acid/CO₂. *ACS Catal.* **2018**, *8*, 2277–2285. [[CrossRef](#)]
43. Hao, P.; Schwartz, D.K.; Medlin, J.W. Effect of Surface Hydrophobicity of Pd/Al₂O₃ on Vanillin Hydrodeoxygenation in a Water/Oil System. *ACS Catal.* **2018**, *8*, 11165–11173. [[CrossRef](#)]
44. Sun, Q.; Fu, X.; Si, R.; Wang, C.-H.; Yan, N. Mesoporous Silica-Encaged Ultrafine Bimetallic Nanocatalysts for CO₂ Hydrogenation to Formates. *ChemCatChem* **2019**, *11*, 5093–5097. [[CrossRef](#)]
45. Umegaki, T.; Satomi, Y.; Kojima, Y. Catalytic Properties of Palladium Nanoparticles for Hydrogenation of Carbon Dioxide into Formic Acid. *J. Jpn. Inst. Energy* **2019**, *96*, 487–492. [[CrossRef](#)]
46. Yang, G.; Kuwahara, Y.; Mori, K.; Louis, C.; Yamashita, H. PdAg alloy nanoparticles encapsulated in N-doped microporous hollow carbon spheres for hydrogenation of CO₂ to formate. *Appl. Catal. B Environ.* **2011**, *283*, 119628. [[CrossRef](#)]
47. Chen, Q.; Yakovlev, N.L. Adsorption and interaction of organosilanes on TiO₂ nanoparticles. *Appl. Surf. Sci.* **2010**, *257*, 1395–1400. [[CrossRef](#)]

48. Meroni, D.; Lo Presti, L.; Di Liberto, G.; Ceotto, M.; Acres, R.G.; Prince, K.C.; Bellani, R.; Soliveri, G.; Ardizzone, S. A Close Look at the Structure of the TiO₂-APTES Interface in Hybrid Nanomaterials and Its Degradation Pathway: An Experimental and Theoretical Study. *J. Phys. Chem. C* **2017**, *121*, 430–440. [[CrossRef](#)] [[PubMed](#)]
49. Schmitt, C. Surface Modification of Oxide Nanoparticles Using Phosphonic Acids: Characterization, Surface Dynamics, and Dispersion in Sols and Nanocomposites. Material Chemistry. Ph.D. Thesis, Université Montpellier, Montpellier, France, 2015.
50. Glaser, A.; Foisner, J.; Hoffmann, H.; Friedbacher, G. Investigation of the Role of the Interplay between Water and Temperature on the Growth of Alkylsiloxane Submonolayers on Silicon. *Langmuir* **2004**, *20*, 5599–5604. [[CrossRef](#)] [[PubMed](#)]
51. Klaysri, R.; Tubchareon, T.; Praserttham, P. One-step synthesis of amine-functionalized TiO₂ surface for photocatalytic decolorization under visible light irradiation. *J. Ind. Eng. Chem.* **2017**, *45*, 229–236. [[CrossRef](#)]
52. Cheng, F.; Sajedin, S.M.; Kelly, S.M.; Lee, A.F.; Kornherr, A. UV-stable paper coated with APTES-modified P25 TiO₂ nanoparticles. *Carbohydr. Polym.* **2014**, *114*, 246–252. [[CrossRef](#)]
53. Sharma, R.K.; Yadav, M.; Gaur, R.; Gupta, R.; Adholeya, A.; Gawande, M.B. Synthesis of Iron Oxide Palladium Nanoparticles and Their Catalytic Applications for Direct Coupling of Acyl Chlorides with Alkynes. *ChemPlusChem* **2016**, *81*, 1312–1319. [[CrossRef](#)]
54. Demirelli, M.; Karaoğlu, E.; Baykal, A.; Sözeri, H.; Uysal, E. Synthesis, characterization and catalytic activity of CoFe₂O₄-APTES-Pd magnetic recyclable catalyst. *J. Alloys Compd.* **2014**, *582*, 201–207. [[CrossRef](#)]
55. Didas, S.A.; Choi, S.; Chaikittisilp, W.; Jones, C.W. Amine–Oxide Hybrid Materials for CO₂ Capture from Ambient Air. *Acc. Chem. Res.* **2015**, *48*, 2680–2687. [[CrossRef](#)]
56. Liu, Q.; Yang, X.; Huang, Y.; Xu, S.; Su, X.; Pan, X.; Xu, J.; Wang, A.; Liang, C.; Wang, X.; et al. A Schiff base modified gold catalyst for green and efficient H₂ production from formic acid. *Energy Environ. Sci.* **2015**, *8*, 3204–3207. [[CrossRef](#)]
57. Liu, Q.; Yang, X.; Li, L.; Miao, S.; Li, Y.; Li, Y.; Wang, X.; Huang, Y.; Zhang, T. Direct catalytic hydrogenation of CO₂ to formate over a Schiff-base-mediated gold nanocatalyst. *Nat. Commun.* **2017**, *8*, 1407. [[CrossRef](#)] [[PubMed](#)]
58. Mori, K.; Masuda, S.; Tanaka, H.; Yoshizawa, K.; Chee, M.; Yamashita, H. Phenylamine-functionalized mesoporous silica supported PdAg nanoparticles: A dual heterogeneous catalyst for formic acid/CO₂-mediated chemical hydrogen delivery/storage. *Chem. Commun.* **2017**, *53*, 4677–4680. [[CrossRef](#)] [[PubMed](#)]
59. Srivastava, V. Amine-Functionalized SBA-15 Supported Ru Nanocatalyst for the Hydrogenation CO₂ to Formic Acid. *Catal. Surv. Asia* **2021**, *25*, 192–205. [[CrossRef](#)]
60. Gindri, I.M.; Frizzo, C.P.; Bender, C.R.; Tier, A.Z.; Martins, M.A.P.; Villetti, M.A.; Machado, G.; Rodriguez, L.C.; Rodrigues, D.C. Preparation of TiO₂ Nanoparticles Coated with Ionic Liquids: A Supramolecular Approach. *ACS Appl. Mater. Interfaces* **2014**, *6*, 11536–11543. [[CrossRef](#)] [[PubMed](#)]
61. Xin, B.; Hao, J. Imidazolium-based ionic liquids grafted on solid surfaces. *Chem. Soc. Rev.* **2014**, *43*, 7171–7187. [[CrossRef](#)] [[PubMed](#)]
62. Gurau, G.; Rodríguez, H.; Kelley, S.P.; Janiczek, P.; Kalb, R.S.; Rogers, R.D. Demonstration of Chemisorption of Carbon Dioxide in 1,3-Dialkylimidazolium Acetate Ionic Liquids. *Angew. Chem. Int. Ed.* **2011**, *50*, 12024–12026. [[CrossRef](#)]
63. Wu, Y.; Zhao, Y.; Wang, H.; Yu, B.; Yu, X.; Zhang, H.; Liu, Z. 110th Anniversary: Ionic Liquid Promoted CO₂ Hydrogenation to Free Formic Acid over Pd/C. *Ind. Eng. Chem. Res.* **2019**, *58*, 6333–6339. [[CrossRef](#)]
64. Qadir, M.I.; Weillhard, A.; Fernandes, J.A.; de Pedro, I.; Vieira, B.J.C.; Waerenborgh, J.C.; Dupont, J. Selective Carbon Dioxide Hydrogenation Driven by Ferromagnetic RuFe Nanoparticles in Ionic Liquids. *ACS Catal.* **2018**, *8*, 1621–1627. [[CrossRef](#)]
65. Bordet, A.; Moos, G.; Welsh, C.; Licence, P.; Luska, K.L.; Leitner, W. Molecular Control of the Catalytic Properties of Rhodium Nanoparticles in Supported Ionic Liquid Phase (SILP) Systems. *ACS Catal.* **2020**, *10*, 13904–13912. [[CrossRef](#)]
66. Moos, G.; Emondts, M.; Bordet, A.; Leitner, W. Selective Hydrogenation and Hydrodeoxygenation of Aromatic Ketones to Cyclohexane Derivatives Using a Rh@SILP Catalyst. *Angew. Chem. Int. Ed.* **2020**, *59*, 11977–11983. [[CrossRef](#)]
67. Rengshausen, S.; Van Stappen, C.; Levin, N.; Tricard, S.; Luska, K.L.; DeBeer, S.; Chaudret, B.; Bordet, A.; Leitner, W. Organometallic Synthesis of Bimetallic Cobalt-Rhodium Nanoparticles in Supported Ionic Liquid Phases (Co_xRh_{100-x}@SILP) as Catalysts for the Selective Hydrogenation of Multifunctional Aromatic Substrates. *Small* **2021**, *17*, 2006683. [[CrossRef](#)]
68. Offner-Marko, L.; Bordet, A.; Moos, G.; Tricard, S.; Rengshausen, S.; Chaudret, B.; Luska, K.L.; Leitner, W. Bimetallic Nanoparticles in Supported Ionic Liquid Phases as Multifunctional Catalysts for the Selective Hydrodeoxygenation of Aromatic Substrates. *Angew. Chem. Int. Ed.* **2018**, *57*, 12721–12726. [[CrossRef](#)] [[PubMed](#)]
69. Luska, K.L.; Bordet, A.; Tricard, S.; Sinev, I.; Grünert, W.; Chaudret, B.; Leitner, W. Enhancing the Catalytic Properties of Ruthenium Nanoparticle-SILP Catalysts by Dilution with Iron. *ACS Catal.* **2016**, *6*, 3719–3726. [[CrossRef](#)]
70. Goclik, L.; Offner-Marko, L.; Bordet, A.; Leitner, W. Selective hydrodeoxygenation of hydroxyacetophenones to ethyl-substituted phenol derivatives using a FeRu@SILP catalyst. *Chem. Commun.* **2020**, *56*, 9509–9512. [[CrossRef](#)]
71. Luska, K.L.; Julis, J.; Stavitski, E.; Zakharov, D.N.; Adams, A.; Leitner, W. Bifunctional nanoparticle-SILP catalysts (NPs@SILP) for the selective deoxygenation of biomass substrates. *Chem. Sci.* **2014**, *5*, 4895–4905. [[CrossRef](#)]
72. El Sayed, S.; Bordet, A.; Weidenthaler, C.; Hetaba, W.; Luska, K.L.; Leitner, W. Selective Hydrogenation of Benzofurans Using Ruthenium Nanoparticles in Lewis Acid-Modified Ruthenium-Supported Ionic Liquid Phases. *ACS Catal.* **2020**, *10*, 2124–2130. [[CrossRef](#)]
73. Bordet, A.; El Sayed, S.; Sanger, M.; Boniface, K.J.; Kalsi, D.; Luska, K.L.; Jessop, P.G.; Leitner, W. Selectivity control in hydrogenation through adaptive catalysis using ruthenium nanoparticles on a CO₂-responsive support. *Nat. Chem.* **2021**, *13*, 916–922. [[CrossRef](#)]

74. Bordet, A.; Leitner, W. Metal Nanoparticles Immobilized on Molecularly Modified Surfaces: Versatile Catalytic Systems for Controlled Hydrogenation and Hydrogenolysis. *Acc. Chem. Res.* **2021**, *54*, 2144–2157. [[CrossRef](#)] [[PubMed](#)]
75. Louis Anandaraj, S.J.; Kang, L.; DeBeer, S.; Bordet, A.; Leitner, W. Catalytic Hydrogenation of CO₂ to Formate Using Ruthenium Nanoparticles Immobilized on Supported Ionic Liquid Phases. *Small* **2023**, *19*, 2206806. [[CrossRef](#)] [[PubMed](#)]
76. Philippot, K.; Chaudret, B. Organometallic approach to the synthesis and surface reactivity of noble metal nanoparticles. *C. R. Chim.* **2003**, *6*, 1019–1034. [[CrossRef](#)]
77. Feng, B.; Zhang, Z.; Wang, J.; Yang, D.; Li, Q.; Liu, Y.; Gai, H.; Huang, T.; Song, H. Synthesis of hydrophobic Pd-poly(ionic liquid)s with excellent CO₂ affinity to efficiently catalyze CO₂ hydrogenation to formic acid. *Fuel* **2022**, *325*, 124853. [[CrossRef](#)]
78. Li, Q.; Huang, T.; Zhang, Z.; Xiao, M.; Gai, H.; Zhou, Y.; Song, H. Highly Efficient Hydrogenation of CO₂ to Formic Acid over Palladium Supported on Dication Poly(ionic liquid)s. *Mol. Catal.* **2021**, *509*, 111644. [[CrossRef](#)]
79. Queffelec, C.; Petit, M.; Janvier, P.; Knight, D.A.; Bujoli, B. Surface Modification Using Phosphonic Acids and Esters. *Chem. Rev.* **2012**, *112*, 3777–3807. [[CrossRef](#)] [[PubMed](#)]
80. Fernández-Martínez, M.D.; Godard, C. Hydrogenation of CO₂ into Formates by Ligand-Capped Palladium Heterogeneous Catalysts. *ChemCatChem* **2023**, *15*, e202201408. [[CrossRef](#)]
81. Wanag, A.; Sienkiewicz, A.; Rokicka-Konieczna, P.; Kusiak-Nejman, E.; Morawski, A.W. Influence of modification of titanium dioxide by silane coupling agents on the photocatalytic activity and stability. *J. Environ. Chem. Eng.* **2020**, *8*, 103917. [[CrossRef](#)]
82. Kim, Y.; Lee, H.; Yang, S.; Lee, J.; Kim, H.; Hwang, S.; Jeon, S.W.; Kim, D.H. Ultrafine Pd nanoparticles on amine-functionalized carbon nanotubes for hydrogen production from formic acid. *J. Catal.* **2021**, *404*, 324–333. [[CrossRef](#)]
83. Masuda, S.; Mori, K.; Kuwahara, Y.; Yamashita, H. PdAg nanoparticles supported on resorcinol-formaldehyde polymers containing amine groups: The promotional effect of phenylamine moieties on CO₂ transformation to formic acid. *J. Mater. Chem. A* **2019**, *7*, 16356–16363. [[CrossRef](#)]
84. Wen, M.; Mori, K.; Futamura, Y.; Kuwahara, Y.; Navlani-García, M.; An, T.; Yamashita, H. PdAg Nanoparticles within Core-Shell Structured Zeolitic Imidazolate Framework as a Dual Catalyst for Formic Acid-based Hydrogen Storage/Production. *Sci. Rep.* **2019**, *9*, 15675. [[CrossRef](#)] [[PubMed](#)]
85. Price, T.L., Jr.; Choi, U.H.; Schoonover, D.V.; Arunachalam, M.; Xie, R.; Lyle, S.; Colby, R.H.; Gibson, H.W. Ion Conducting ROMP Monomers Based on (Oxa)norbornenes with Pendant Imidazolium Salts Connected via Oligo(oxyethylene) Units and with Oligo(ethyleneoxy) Terminal Moieties. *Macromolecules* **2019**, *52*, 1371–1388.
86. Dou, Q.; Liu, L.; Yang, B.; Lang, J.; Yan, X. Silica-grafted ionic liquids for revealing the respective charging behaviors of cations and anions in supercapacitors. *Nat. Commun.* **2017**, *8*, 2188. [[CrossRef](#)] [[PubMed](#)]
87. Li, J.R.; Chen, C.; Hu, Y.L. Novel and Efficient Knoevenagel Condensation over Mesoporous SBA-15 Supported Acetate-functionalized Basic Ionic Liquid Catalyst. *ChemistrySelect* **2020**, *5*, 14578–14582.
88. Dai, Y.; Wang, S.; Wu, J.; Tang, J.; Tang, W. Dicationic AC regioisomer cyclodextrins: Mono-6^A-ammonium-6^C-alkylimidazolium-β-cyclodextrin chlorides as chiral selectors for enantioseparation. *RSC Adv.* **2012**, *2*, 12652–12656. [[CrossRef](#)]
89. Roshan, K.R.; Mathai, G.; Kim, J.; Tharun, J.; Park, G.-A.; Park, D.-W. A biopolymer mediated efficient synthesis of cyclic carbonates from epoxides and carbon dioxide. *Green Chem.* **2012**, *14*, 2933. [[CrossRef](#)]
90. Brodard-Severac, F.; Guerrero, G.; Maquet, J.; Florian, P.; Gervais, C.; Mutin, P.H. High-Field ¹⁷O MAS NMR Investigation of Phosphonic Acid Monolayers on Titania. *Chem. Mater.* **2008**, *20*, 5191–5196. [[CrossRef](#)]
91. Zhang, J.; Deo, S.; Janik, M.J.; Medlin, J.W. Control of Molecular Bonding Strength on Metal Catalysts with Organic Monolayers for CO₂ Reduction. *J. Am. Chem. Soc.* **2020**, *142*, 5184–5193. [[CrossRef](#)]
92. Helmy, R.; Fadeev, A.Y. Self-Assembled Monolayers Supported on TiO₂: Comparison of C₁₈H₃₇SiX₃ (X = H, Cl, OCH₃), C₁₈H₃₇Si(CH₃)₂Cl, and C₁₈H₃₇PO(OH)₂. *Langmuir* **2002**, *18*, 8924–8928. [[CrossRef](#)]

Disclaimer/Publisher's Note: The statements, opinions and data contained in all publications are solely those of the individual author(s) and contributor(s) and not of MDPI and/or the editor(s). MDPI and/or the editor(s) disclaim responsibility for any injury to people or property resulting from any ideas, methods, instructions or products referred to in the content.